Variational approach to finite-temperature magnetism. II. Antiferromagnetism

Y. Kakehashi and J. H. Samson
Max-Planck-Institut für Festkörperforschung, D-7000 Stuttgart 80, Federal Republic of Germany
(Received 13 August 1985)

The overall features of a variational theory for finite-temperature magnetism, which has recently been proposed, are investigated numerically for a half-filled Hubbard model. The phase diagram, sublattice magnetization, staggered susceptibility, amplitude of local moments, charge fluctuations, and electronic contributions to the internal energy, entropy, and the thermal expansion are calculated as functions of temperature T and the Coulomb interaction U. It is found that the local electron correlations, which cannot be described by the static approximation to the functional integral, act so as to reduce the effective Coulomb interaction for the magnetization, the Néel temperature, the internal energy, the specific heat, and the entropy, while they enhance the atomic character for the amplitude of local moments, the charge fluctuation, and the reduced-magnetization—versus—temperature curves. Electron correlations reduce the thermal expansion, in contrast to the case of ferromagnets.

I. INTRODUCTION

It is well known that electron correlations are important in transition metals and compounds. The correlations reduce the stability of magnetic long-range order as compared with the Hartree-Fock approximation for the ground state,[1-4] give rise to a metal-insulator transition,[2,3,5,6] strongly reduce the cohesive energy and bulk modulus,[7,8] and enhance the amplitude of the local magnetic moment.[8-10] These effects of electron correlations which are seen in the ground state also play important roles even at finite temperatures since the energy gain due to the correlated motion of electrons is usually much larger than the Curie (Néel) temperature T_C (T_N).

A useful technique for investigating finite-temperature magnetism in transition metals and alloys is the functional-integral method, in which an interacting electron system is transformed into a one-electron system in a time-dependent field $\{\xi_i(\tau)\}$.[11,12] This method allows for the description of local-moment features as well as band features.[13-15] Numerical calculations[16-21] are limited to the static approximation, where the time-dependent field variables $\{\xi_i(\tau)\}$ are replaced by static ones $\{\xi_i=\beta^{-1}\int_0^\beta \xi_i(\tau)d\tau\}$. Here β is the inverse temperature, $1/k_BT$. This is valid in the high-temperature limit. At $T=0$ the approximation reduces to Hartree-Fock theory. Thus, the electron-correlation effects mentioned above are not sufficiently taken into account. We have, therefore, recently developed a theory to treat the correlations on the basis of a variational principle.[22] In this theory the free energy reduces to a Gutzwiller-type variational energy[2,8,10] at $T=0$, and it agrees with the free energy in the static approximation at high temperatures, as it should.

Some numerical calculations for Fe and Ni have been described in the previous paper[22] (which is referred to as I in the following). A large reduction of T_C was found for Fe in the model calculation. It was also found that the amplitude of local moments is almost temperature independent below and above T_C.

The purpose of this paper is to present numerical results for a half-filled band in order to show the overall features of the variational theory. Antiferromagnetism is favored in a half-filled band. The effect of local electron correlations on the two-sublattice antiferromagnetic ground state has been investigated by Ogawa and Kanda[23] for the single-band case and Oleś[24] for the degenerate-band case by means of a Gutzwiller-type variational approach. In this case it is found that the electron-correlation effects are not very significant, since the Hartree-Fock exchange splitting itself reduces the probability of double occupancy of electrons on a site and partially includes the Hund's-rule coupling. Takano and Okiji[25] have reported some interesting results for the metal-insulator transition, taking the degeneracy into account.

Antiferromagnetism has been investigated at finite temperatures by several authors within the static approximation.[13,17,18,26] We discuss in this paper the effect of local electron correlations on various quantities as a function of temperature and Coulomb interaction.

First, we briefly review in the following section the variational theory within the single-site approximation (SSA). The numerical results are presented in Sec. III. The sublattice magnetization, staggered susceptibility, phase diagram, amplitude of local moments, charge fluctuations, internal energy, entropy, and the electronic contribution to the thermal expansion are calculated as functions of temperature T and the Coulomb interaction U. The effects of local electron correlation on these quantities are found in the small- and intermediate-coupling regime $0<U/W\lesssim 1$, where W is the d-band width. Physical reasons for these effects are also given. Finally, a summary is presented in the last section.

II. REVIEW OF THE VARIATIONAL THEORY

Our treatment of electron correlation at finite temperatures is based on the physical assumption that the energy gain due to correlated motion of electrons is much larger

than the Curie temperature (T_C) or the Néel temperature (T_N). This condition is satisfied in the transition metals. Then we may include adiabatically that part of the electron correlations which is not described within the static approximation to the functional integral.

We adopt the single-band Hubbard model for brevity:

$$H=\sum_{i,\sigma}\varepsilon^0 n_{i\sigma}+\sum_{i,j,\sigma}t_{ij}a^{\dagger}_{i\sigma}a_{j\sigma}+\sum_i U n_{i\uparrow}n_{i\downarrow}\ . \tag{2.1}$$

Here ε^0 is the atomic level. The transfer integral between sites i and j is denoted by t_{ij}. U is the Coulomb integral. $a^{\dagger}_{i\sigma}$ ($a_{i\sigma}$) is the creation (annihilation) operator on site i with spin σ, and $n_{i\sigma}=a^{\dagger}_{i\sigma}a_{i\sigma}$.

The formulation is based on Feynman's variational principle for the exact free energy F expressed in the functional-integral formalism,

$$F\leqq F_t+\langle E(\xi,T)-E_t(\xi,T)\rangle_t\ , \tag{2.2}$$

$$e^{-\beta F}=\left[\frac{\beta U}{4\pi}\right]^{N/2}\int\left[\prod_i d\xi_i\right]e^{-\beta E(\xi,T)}\ , \tag{2.3}$$

$$\langle(\cdots)\rangle_t\equiv\frac{\int\left[\prod_i d\xi_i\right]e^{-\beta E_t}(\cdots)}{\int\left[\prod_i d\xi_i\right]e^{-\beta E_t}}\ , \tag{2.4}$$

where ξ stands for the exchange field $\xi_1,\xi_2,\ldots,\xi_N$, and N is the number of sites. $E(\xi,T)$ denotes an exact energy functional. The charge-field variables and the finite-frequency components of the exchange field have been formally integrated out [see Eq. (2.3) in paper I]. F_t is defined by Eq. (2.3) with $E(\xi,T)$ replaced by a trial energy functional $E_t(\xi,T)$. The latter is assumed to be

$$E_{\rm st}(\xi,\zeta(\xi))+E_c(\xi,\zeta(\xi),\eta(\xi))$$

(see Ref. 22.) Here $E_{\rm st}(\xi,\zeta(\xi))$ is the energy functional in the static approximation,[17,20] and $E_c(\xi,\zeta(\xi),\eta(\xi))$ is the correlation energy of the ground state in the exchange field (ξ_i) as determined in the Gutzwiller scheme. $\{\zeta_i(\xi)\}$ and $\{\eta_i(\xi)\}$ are variational parameters describing a charge potential and correlated motion of electrons, respectively. They are determined by the variational principle [Eq. (2.2)].

We assume a two-sublattice antiferromagnetic state with one "up" and one "down" site per unit cell. Then all sites are equivalent and the energy functional in the SSA is given by

$$E_G(\xi,\zeta,\eta)=E_{\rm st}(\xi,\zeta(\xi))+E_c(\xi,\zeta(\xi),\eta(\xi))\ , \tag{2.5}$$

$$\begin{aligned}E_{\rm st}(\xi,\zeta(\xi))=&\int d\omega f(\omega)\frac{1}{\pi}{\rm Im}\\&\times\sum_\sigma\ln\{[L_\sigma(\omega,\xi)]^{-1}-[\mathscr{L}_\sigma(\omega)]^{-1}\\&+[F_\sigma(\omega)]^{-1}\}\\&-\tfrac{1}{4}U([\zeta(\xi)]^2-\xi^2)\ ,\end{aligned} \tag{2.6}$$

$$E_c(\xi,\zeta(\xi),\eta(\xi))=\frac{-2\eta\langle O\tilde{H}\rangle_0+\eta^2\langle O\tilde{H}O\rangle_0}{1+\eta^2\langle O^2\rangle_0}\ . \tag{2.7}$$

Here the site index has been omitted. $f(\omega)$ is the Fermi distribution function and $[\mathscr{L}_\sigma(\omega)]^{-1}$ is the effective medium for spin σ on the $(+)$ sublattice, to be determined self-consistently later [see Eq. (2.19)]. The locator $L_\sigma(\omega,\xi)$ is defined by

$$[L_\sigma(\omega,\xi)]^{-1}=\omega-[\varepsilon^0-\mu+\tfrac{1}{2}U\zeta(\xi)-\tfrac{1}{2}U\xi\sigma]\ . \tag{2.8}$$

$F_\sigma(\omega)$ in Eq. (2.6) is the coherent Green function on the $(+)$ sublattice. It is given by[27,28]

$$\begin{aligned}F_\sigma(\omega)=&\left[\frac{[\mathscr{L}_{-\sigma}(\omega)]^{-1}}{[\mathscr{L}_\sigma(\omega)]^{-1}}\right]^{1/2}\\&\times\int\frac{\rho_0(\varepsilon)}{\{[\mathscr{L}_+(\omega)]^{-1}[\mathscr{L}_-(\omega)]^{-1}\}^{1/2}-\varepsilon}d\varepsilon\end{aligned} \tag{2.9}$$

if $\varepsilon_{\mathbf{k}}=-\varepsilon_{\mathbf{k}+\mathbf{Q}}$ for all $\mathbf{k}$ in the Brillouin zone, $\mathbf{Q}$ being $2\pi(1,0,0)/a$ in the case of a cubic lattice, where a is the lattice parameter of a unit cell with cubic symmetry. $\rho_0(\varepsilon)$ in Eq. (2.9) is the density of states (DOS) of the noninteracting system.

The operator O in Eq. (2.7) is

$$(n_\uparrow-\langle n_\uparrow\rangle_0)(n_\downarrow-\langle n_\downarrow\rangle_0)\ ,$$

and $\tilde{H}\equiv H-\langle H\rangle_0$.[8-10] The average $\langle\cdots\rangle_0$ is taken with respect to the one-electron Hamiltonian $H^0(\xi)$ in the static approximation. This is given by

$$\begin{aligned}H^0(\xi)=&\sum_{i,\sigma}[\varepsilon^0-\mu+\tfrac{1}{2}U\zeta_i(\xi)-\tfrac{1}{2}U\xi_i\sigma]n_{i\sigma}\\&+\sum_{i,j,\sigma}t_{ij}a^{\dagger}_{i\sigma}a_{j\sigma}\ .\end{aligned} \tag{2.10}$$

The expressions for $\langle O^2\rangle_0$, $\langle O\tilde{H}\rangle_0$, and $\langle O\tilde{H}O\rangle_0$ are given in Appendix B in paper I. The variational parameter $\eta(\xi)$ is obtained analytically in the present case as follows:

$$\eta(\xi)=\frac{-\langle O\tilde{H}O\rangle_0+(\langle O\tilde{H}O\rangle_0^2+4\langle O\tilde{H}\rangle_0^2\langle O^2\rangle_0)^{1/2}}{2\langle O\tilde{H}\rangle_0\langle O^2\rangle_0}\ . \tag{2.11}$$

The charge potential $\zeta(\xi)$ has to be obtained numerically from the variational equation $\partial E_G(\xi,\zeta,\eta)/\partial\zeta=0$. In the following calculations, however, we have approximated it by that of the static approximation,

$$\zeta(\xi)=n^0(\xi)\ , \tag{2.12}$$

where $n^0(\xi)$ is the local charge on a site resulting from the one-electron Hamiltonian $H^0(\xi)$.

The free energy per atom is expressed as

$$F_G=\langle H\rangle-TS\ . \tag{2.13}$$

The energy $\langle H\rangle$ and entropy S are given by

$$\langle H\rangle=\mu n+\int d\omega f(\omega)\omega\langle\rho(\omega\xi)\rangle-\tfrac{1}{4}U\{\langle[\zeta(\xi)]^2\rangle-\langle\xi^2\rangle+2/\beta U\}+\langle E_C(\xi,\eta(\xi))\rangle\ , \tag{2.14}$$

$$S=-\int d\omega\langle\rho(\omega\xi)\rangle\{[1-f(\omega)]\ln[1-f(\omega)]+f(\omega)\ln f(\omega)\}+\ln\int d\xi\left[\frac{\beta U}{4\pi}\right]^{1/2}e^{-\beta(E_G-\langle E_G\rangle)}-\tfrac{1}{2}\ . \tag{2.15}$$

Here $\rho(\omega\xi)$ is the local DOS on a site for the one-electron Hamiltonian (2.10). The average $\langle\cdots\rangle$ on the right-hand side (rhs) in Eqs. (2.14) and (2.15) is defined by

$$\langle\cdots\rangle=\frac{\int e^{-\beta E_G}(\cdots)d\xi}{\int e^{-\beta E_G}d\xi}\ . \tag{2.16}$$

The first three terms of the rhs in Eq. (2.14) correspond to the energy in the static approximation with a renormalized thermal average (2.16). The last term denotes the correlation energy. The first term in the entropy (2.15) is the entropy of independent fermions with a temperature-dependent DOS $\langle\rho(\omega\xi)\rangle$. The second term describes the magnetic entropy. The last term in Eq. (2.15) is related to the Gaussian prefactor $\sqrt{\beta U/4\pi}$ in the static approximation. The sublattice magnetization $\langle m\rangle$, the thermal averages of the square of the local charge, and the local moment are calculated from

$$\langle m\rangle=\langle\xi\rangle-\left\langle\frac{2\eta^2\langle O^2\rangle_0 m^0(\xi)}{1+\eta^2\langle O^2\rangle_0}\right\rangle\ , \tag{2.17}$$

$$\left.\begin{matrix}\langle m^2\rangle\\ \langle n^2\rangle\end{matrix}\right\}=1\mp\tfrac{1}{2}\left[1-\langle\xi^2\rangle+\frac{2}{\beta U}\right]\pm\left\langle\frac{4\eta\langle O^2\rangle_0}{1+\eta^2\langle O^2\rangle_0}\right\rangle\ . \tag{2.18}$$

Here we have assumed a symmetric half-filled band $\rho(\omega\xi)$, so that $n^0(\xi)=1$. $m^0(\xi)$ is the local magnetization resulting from the one-electron Hamiltonian (2.10).

The effective medium $\mathscr{L}_\sigma^{-1}$ which describes the long-range order is determined by a simplified coherent-potential-approximation (CPA) equation,[17,20]

$$\sum_\nu\frac{1}{2}\left[1+\nu\frac{\langle\xi\rangle}{(\langle\xi^2\rangle)^{1/2}}\right]\{[L_\sigma(\omega\xi)]^{-1}-\mathscr{L}_\sigma^{-1}+F_\sigma^{-1}\}^{-1}=F_\sigma\ , \tag{2.19}$$

$$\left.\begin{matrix}\langle\xi\rangle\\ \langle\xi^2\rangle\end{matrix}\right\}=\int d\xi\left\{\begin{matrix}\xi\\ \xi^2\end{matrix}\right\}\times e^{-\beta E_G}\Big/\int d\xi\, e^{-\beta E_G}\ . \tag{2.20}$$

The parameters $\{[\mathscr{L}_\sigma(\omega)]^{-1},\langle\xi\rangle,\langle\xi^2\rangle\}$ must be obtained by solving Eqs. (2.19) and (2.20) self-consistently.

It should be noted that the parameters $\{\mathscr{L}_\sigma^{-1},\zeta,\eta,\langle\xi\rangle,\langle\xi^2\rangle\}$ obtained by the present Eqs. (2.11), (2.12), (2.19), and (2.20) do not, in general, guarantee stationarity for the free energy in the single-site approximation [Eq. (2.13)]. This does not give rise to serious difficulties in the half-filled case. However, a clear violation of thermodynamic relations and an inconsistent phase stability are seen to occur when the electron number deviates far from 1. In this case we have to determine the parameters $\{\mathscr{L}_\sigma^{-1},\zeta,\eta,\langle\xi\rangle,\langle\xi^2\rangle\}$ directly from the variational principle, so that the stationary condition is satisfied, which would greatly complicate the self-consistent equations.

III. NUMERICAL RESULTS

The numerical calculations are performed on a semielliptical model DOS,

$$\rho_0(\varepsilon)=\begin{cases}(8/\pi W)(W^2/4-\varepsilon^2)^{1/2}, & |\varepsilon|\leqq W/2\\ 0, & |\varepsilon|>W/2\end{cases} \tag{3.1}$$

where W is the bandwidth. The Fermi distribution function is neglected as in the previous calculations.

The ground-state properties in the present theory are summarized in Fig. 1. The ground state is antiferromagnetic for an arbitrarily small Coulomb interaction, since perfect nesting at the Fermi level causes a large kinetic-energy gain. The local electron correlations reduce the Hartree-Fock magnetization by 5—20% in the intermediate regime $0<U/W\lesssim 1$. For large values of U a large Hartree-Fock exchange splitting strongly decreases the probability of double occupancy of electrons on a site, so that the correlation-energy gain $-\langle E_c\rangle$ becomes smaller.

The contribution of quantum fluctuations to the amplitude of local moments is taken into account in the present calculation.[22] Thus the amplitude of local moments, $\langle m^2\rangle^{1/2}$, takes the correct value $1/\sqrt{2}$ at $U=0$, while it vanishes for $U=0$ in the previous calculation.[17] The amplitude gradually increases with increasing U, approaching the correct atomic limit ($1\mu_B$). On the other hand, the charge fluctuations decrease with increasing U, and vanish at $U/W=\infty$ as they should. The local electron correlations enhance the amplitude of local moments and suppress the charge fluctuation ($[\langle(\delta n)^2\rangle]^{1/2}$) by several

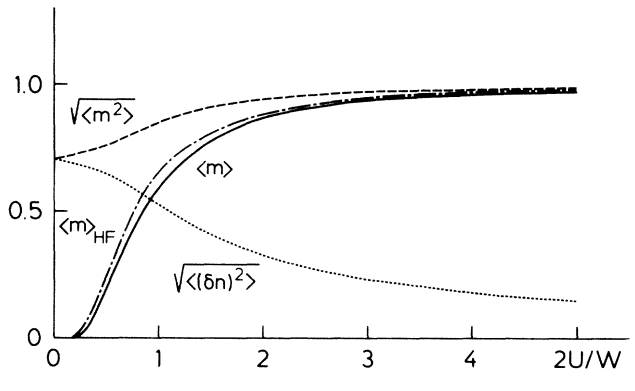

FIG. 1. Ground-state sublattice magnetization $\langle m\rangle$, the root-mean-square value of local moments $(\langle m^2\rangle)^{1/2}$, and the charge fluctuation $[\langle(\delta n)^2\rangle]^{1/2}$ as a function of the Coulomb interaction U divided by the half-bandwidth $W/2$. Dotted-dashed curves ($\langle m\rangle_{\rm HF}$) show the ground-state sublattice magnetization in the Hartree-Fock approximation.

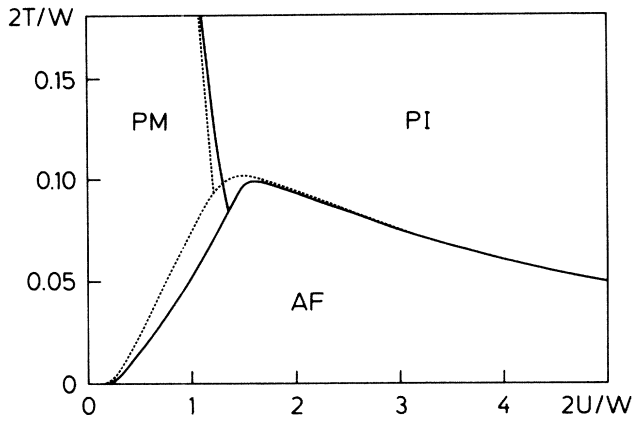

FIG. 2. Magnetic phase diagram for the half-filled band, showing the paramagnetic metal (PM), the paramagnetic insulator (PI), and the antiferromagnetic state (AF). Solid (dotted) lines show the phase boundary in the variational approach (the static approximation).

percent in the intermediate regime.

The interpolation character of the present theory can be seen in the phase diagram in Fig. 2. The Néel temperature increases with increasing U, and has a maximum at $2U/W \simeq 1.6$. In the intermediate regime $0 < 2U/W \lesssim 2$ the Néel temperature is reduced because of the local electron correlations. There is no reduction of T_N in the regime $2U/W \gg 1$ since the present theory reduces to the static approximation in the weak and strong Coulomb interaction regimes. The present theory reduces to the molecular-field approximation for the spin-$\frac{1}{2}$ Heisenberg model in the regime $2U/W \gg 1$.

The phase boundary between the paramagnetic metal (PM) and the paramagnetic insulator (PI) is defined by the line along which a gap appears in the CPA density of states. The local electron correlations effectively reduce the Coulomb interaction in the exchange potential $-\frac{1}{2}U\xi\sigma$. Thus the phase boundary is shifted slightly towards the insulator regime. It should be noted that the metal-insulator phase boundary defined here is a conventional one to indicate a transition regime from a metal to an insulator; we do not obtain such a gap at finite temperatures when we use instead of Eq. (2.19) the full CPA equation,[16,29,30] allowing for a continuous exchange-field distribution. A high-temperature expansion also shows a gradual transition from a metal to an insulator in the paramagnetic regime.[31]

Figures 3(a) and 3(b) show the energy functional for various values of U in the paramagnetic state. The correlation energy functional $E_c(\xi)$ has a minimum at $\xi=0$, which deepens with increasing U. For large U a local minimum appears in the total energy functional at $\xi=0$. The depth of the minimum in $E_c(\xi)$ is $-U/4$ in the atomic limit. However, the width of the well becomes zero in this limit, so that there is no electron-correlation correction to any physical quantities. Thus, correlation corrections appear only in the intermediate regime. In the antiferromagnetic state the minimum of E_c shifts so as to reduce the local magnetization.

The magnetization-versus-temperature curves are shown in Fig. 4 for various values of U. The reduction of

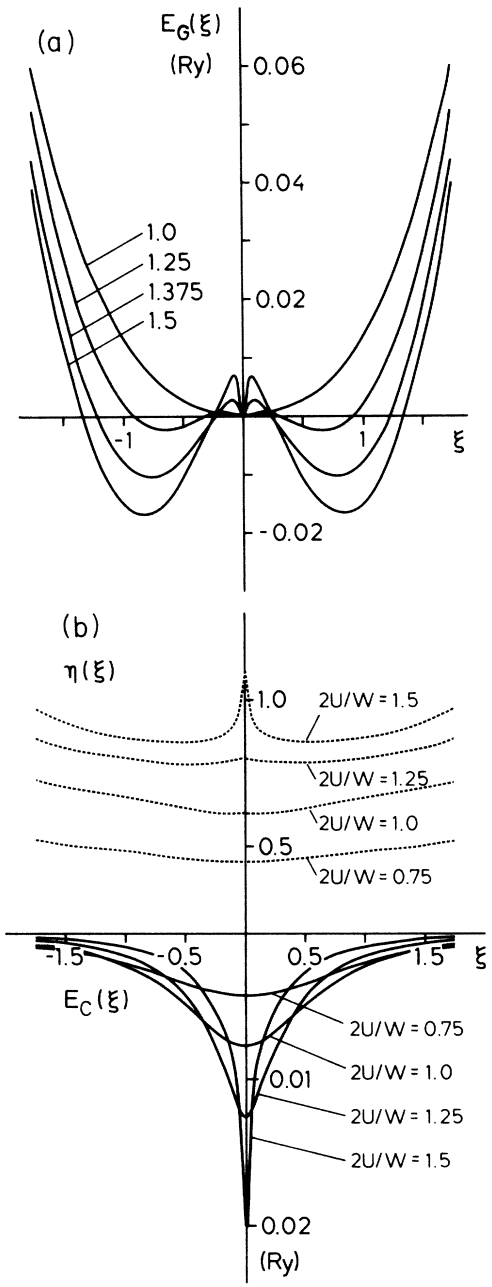

FIG. 3. (a) Energy functional $E_G(\xi)$ in the single-site approximation for various Coulomb interactions $U/W=1.0$, 1.25, 1.375, and 1.5. (b) Local correlation parameters $\eta(\xi)$ and correlation energy functionals for various Coulomb interactions.

the Néel temperature is largest near $2U/W=1$, where it is about 30%. The local electron correlation reduces the magnetization, but it enhances the atomic character by suppression of charge fluctuations. This is seen in the reduced magnetization curves in Fig. 5. They are closer to the Brillouin form for $S=\frac{1}{2}$ than are those in the static approximation. Evidence for such a correlation effect seems to be seen in the sublattice magnetization curve of Cr, which follows the Brillouin form for spin-$\frac{1}{2}$ in spite of the small value ($0.6\mu_B$) of the sublattice magnetization at $T=0$.[32]

The amplitude of local moments is strongly enhanced

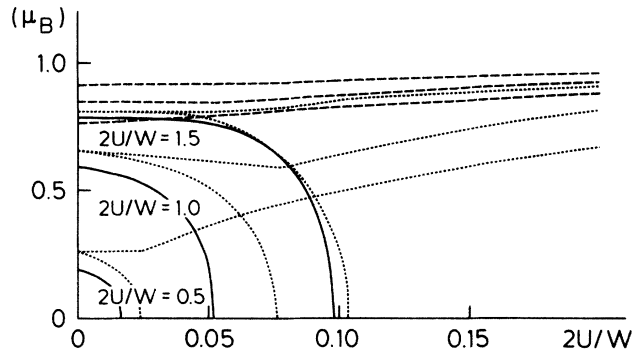

FIG. 4. The temperature dependence of $\langle m \rangle$ and $(\langle m^2 \rangle)^{1/2}$ in the present approximation (solid and dashed curves) and in the static approximation (dotted curves) (Ref. 17).

by the inclusion of the quantum fluctuations as well as the local electron correlations (see Sec. II in paper I). The temperature dependence of the amplitude is very small as compared with that in the static approximation.[17] These discrepancies are particularly large for small $2U/W$ at low temperatures, as shown in Fig. 4.

The correlation correction to the amplitude of local moments changes little in a temperature range of T_N. It vanishes above a temperature $T^* \gtrsim W^2/8U$ for the following reason: The correlation contribution due to double occupancy of electrons on the same site disappears above a temperature T^* where the average exchange splitting is comparable to the d-band width, i.e., $U(\langle \xi^2 \rangle)^{1/2} \sim W$. On the other hand, the characteristic temperature is of the form $T^* \sim U\langle \xi^2 \rangle/4$ when T^* is sufficiently high because the energy functional is approximately quadratic for large $|\xi|$ [see Eq. (2.6)]. Eliminating $(\langle \xi^2 \rangle)^{1/2}$ from the two relations, we obtain $2T^*/W \sim W/4U$. It is 1.0 for $2U/W=0.5$; this is much larger than $2T_N/W$.

The staggered susceptibility follows the Curie-Weiss law, as shown in Fig. 6. The Curie constants are hardly modified by the local correlation, because T^* is much larger than T_N.

The temperature dependence of the internal energy is shown in Fig. 7. The magnetic energy, defined by

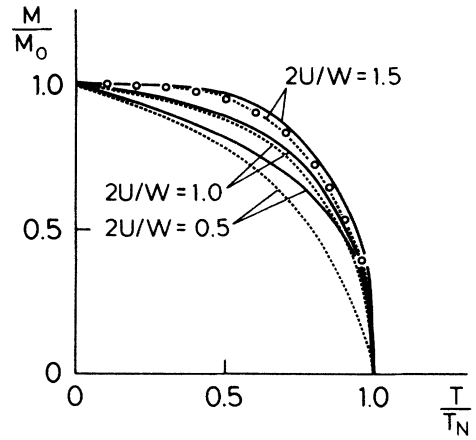

FIG. 5. Reduced sublattice-magnetization curves in the variational approach (solid curves) and in the static approximation (dotted curves). Open circles show the $S=\frac{1}{2}$ Brillouin curve.

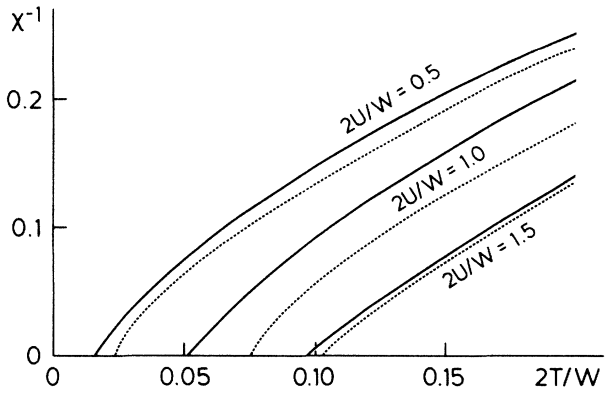

FIG. 6. Inverse staggered susceptibilities for various values of the Coulomb interaction. The solid (dotted) curves show the results in the variational approach (the static approximation).

$$\Delta E_m = \langle H \rangle_{T=T_N} - \langle H \rangle_{T=0} ,$$

increases initially with increasing U and has a maximum. The corresponding specific heat becomes large and shows local-moment behavior for large U. In the present calculation the Fermi distribution function is replaced by a step function, and the CPA equations are also simplified by replacing the probability functional

$$P(\xi) \equiv e^{-\beta E_G(\xi)} \Big/ \int d\xi\, e^{-\beta E_G(\xi)}$$

by a two δ functions. If these are fully treated, we find a large electronic contribution from the Fermi distribution function to the specific heat in the paramagnetic state [see the second term on the rhs in Eq. (2.14)]. The latter usually compensates for the negative specific heat above T_N found in the present calculation.[29]

In the static approximation the energies in the paramagnetic state are generally overestimated more than those in the ferromagnetic state. Therefore, local electron correlations reduce the magnetic energy in the intermediate-coupling regime. This is the main reason for the reduction of T_N.

The magnetic entropy is shown in Fig. 8 as a function

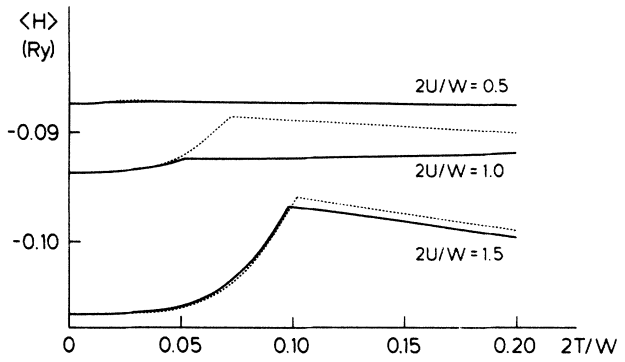

FIG. 7. Temperature dependence of the internal energy in the variational approach (solid curves) and in the static approximation (dotted curves). Energies in the static approximation are shifted down so that they agree with those in the variational approach at $T=0$.

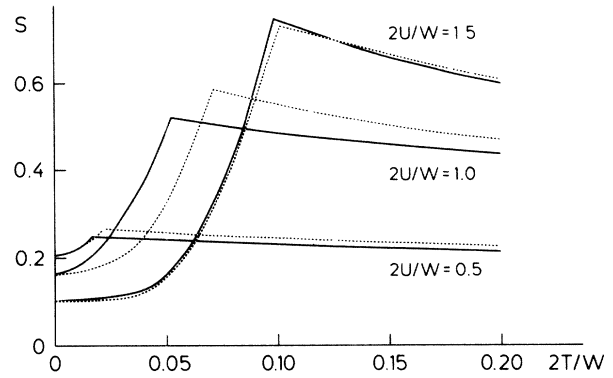

FIG. 8. Temperature dependence of entropies for various Coulomb interactions. The results in the static approximation (dotted curves) are shifted so that the values at $T=0$ agree with those in the variational approach (solid curves).

of U. The characteristic magnetic entropy ΔS_m, which is defined by $S(T_N)-S(T=0)$, increases with increasing U. For $U/W \gg 1$ it reduces to the atomic entropy ln2.

The present theory leads to a residual ground-state entropy in the intermediate regime, as in the static approximation. It is given by

$$S(T=0)=\tfrac{1}{2}\ln\left[\frac{U}{2\partial^2 E_G(\xi^*)/\partial\xi^2}\right] . \tag{3.2}$$

This point may have to be dealt with in the future. The local electron correlations reduce ΔS_m in the intermediate regime in comparison with the static approximation, since the correlated motion of electrons suppresses degrees of freedom.

The temperature dependence of the bonding energy

$$E_b(T)=\left\langle \sum_{i,j,\sigma} t_{ij} a_{i\sigma}^{\dagger} a_{j\sigma} \right\rangle$$

is shown in Fig. 9 for various values of U. The bonding is directly connected with the electron contribution $\alpha_e(T)$ to the thermal-expansion coefficient via the relation[33,34]

$$\alpha_e(T)=\frac{\dot{D}}{3BV}\frac{\partial E_b}{\partial T} , \tag{3.3}$$

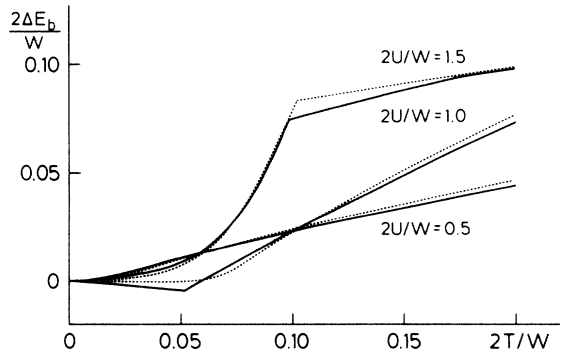

FIG. 9. Temperature dependence of bonding energy $\Delta E_b=E_b(T)-E_b(0)$ in the variational approach (solid curves) and in the static approximation (dotted curves).

where B is the bulk modulus, V is a volume per atom, and $\dot{D}$ is an electronic Grüneisen constant, which can be calculated from Andersen's potential parameters.[33,34-37] [The notation has been changed. $\dot{D}$ is the same as $2\dot{\mathscr{D}}$ in the appendix of Ref. 33 and (D/t) in Refs. 34 and 37.] The volume change due to the electrons between $T=0$ and $T=T_N$ is therefore given by

$$\dot{D}[E_b(T_N)-E_b(0)]/3BV .$$

Here $E_b(T_N)-E_b(0)$ takes the values 0.0003, -0.0010, and 0.0149 Ry for $2U/W=0.5$, 1.0, and 1.5, respectively, in the present theory, while it is 0.0004, 0.0009, and 0.0166 Ry, respectively, in the static approximation. Namely, the local electron correlations act so as to cause a volume contraction with increasing temperature in antiferromagnetic metals. This is seen from the following physical consideration.

Let us consider the case of nearest-neighbor hopping, and assume that the exchange splittings are temperature independent, in order to see the essential features of the effect of electron correlations. The volume contraction is proportional to the electron-hopping rate $\langle a_{i\sigma}^{\dagger} a_{j\sigma}\rangle$, as seen in Eq. (3.3). In the antiferromagnetic ground state the electron correlations suppress the hopping rate because electron hopping to a neighboring empty level creates a doubly occupied state of large energy. Therefore, the electron correlations tend to expand the volume. However, in the paramagnetic state the local moments are aligned at random. Then the number of neighboring empty levels with the same spin as the central electron decreases, and the effect of the volume expansion due to correlation decreases. Therefore, the local-electron-correlation effect decreases the volume with increasing temperature. This is just the opposite of the case of the ferromagnetic metals, where the electron-correlation effects increase the volume with increasing temperature.[38]

IV. SUMMARY

We have performed numerical calculations for the finite-temperature magnetism of a half-filled Hubbard model in order to demonstrate the interpolation character of the variational theory proposed in paper I, and to investigate local-electron-correlation effects on various quantities in the intermediate-coupling regime.

The theory gives a better description of the overall features of finite-temperature magnetism from weak magnetism to strong magnetism. The local correlation effects neglected by the static approximation are not as large in the case of the half-filled band as they are in ferromagnets, but do appear in the weak and intermediate regime ($0<U/W\lesssim 1$). In this regime the magnetization as well as the Néel temperature is reduced by up to 30%, because the static approximation had overestimated the magnetic energy. On the other hand, the local electron correlations suppress charge fluctuations, so that atomic features are enhanced. This is seen in the increased amplitude of local moments and the reduced magnetization. The staggered susceptibility follows a Curie-Weiss law. Calculated effective Bohr-magneton numbers are hardly affected by including the local electron correlations since

this is a high-temperature quantity for which the static approximation works well.

The correlated electron motion lowers the energy in the paramagnetic state more than in the antiferromagnetic state. Therefore the energy is less strongly temperature dependent than that of the static approximation in the intermediate regime. This implies that the specific-heat peaks at T_N are somewhat reduced. The temperature dependence of the entropy is also reduced at temperatures $T \ll T^*$ because the correlated motion of electrons at finite temperatures reduces the effective number of degrees of freedom in the intermediate regime.

The local-electron-correlation effect on the thermal expansion in antiferromagnetic metals is very different from that in ferromagnetic metals. In the latter, the volume increases with increasing temperature, while in the former it decreases. In particular, the electron correlations can change the sign of the spontaneous volume magnetostriction in the intermediate regime ($2U/W \sim 1.0$).

ACKNOWLEDGMENTS

The authors would like to thank Professor P. Fulde for a critical reading of the manuscript and for valuable discussions.

[1]J. H. Van Vleck, Rev. Mod. Phys. **25**, 220 (1953).
[2]M. C. Gutzwiller, Phys. Rev. **134**, A293 (1964); **137**, A1726 (1965).
[3]J. Hubbard, Proc. R. Soc. London, Ser. A **276**, 238 (1963); **277**, 237 (1964); **281**, 401 (1964).
[4]J. Kanamori, Prog. Theor. Phys. **30**, 275 (1963).
[5]N. F. Mott, Proc. Phys. Soc. London, Sect. A **62**, 416 (1949).
[6]W. F. Brinkman and T. M. Rice, Phys. Rev. B **2**, 4302 (1970).
[7]J. Friedel and C. M. Sayers, J. Phys. (Paris) **38**, 697 (1977).
[8]A. M. Oleś, Phys. Rev. B **23**, 271 (1981).
[9]G. Stollhoff and P. Thalmeier, Z. Phys. B **43**, 13 (1981).
[10]A. M. Oleś and G. Stollhoff, Phys. Rev. B **29**, 314 (1984).
[11]R. L. Stratonovich, Dokl. Akad. Nauk SSSR **115**, 1097 (1957) [Sov. Phys.—Dokl. **2**, 416 (1958)].
[12]J. Hubbard, Phys. Rev. Lett. **3**, 77 (1959).
[13]M. Cyrot, Phys. Rev. Lett. **25**, 871 (1970); J. Phys. (Paris) **33**, 125 (1972).
[14]H. Hasegawa, Solid State Commun. **31**, 597 (1979).
[15]T. Moriya and Y. Takahashi, J. Phys. Soc. Jpn. **45**, 397 (1978).
[16]J. Hubbard, Phys. Rev. B **19**, 2626 (1979); **20**, 4584 (1979); **23**, 5970 (1981).
[17]H. Hasegawa, J. Phys. Soc. Jpn. **46**, 1504 (1979); **49**, 178 (1980).
[18]T. Moriya and H. Hasegawa, J. Phys. Soc. Jpn. **48**, 1490 (1980).
[19]K. Usami and T. Moriya, J. Magn. Magn. Mater. **20**, 171 (1980).
[20]Y. Kakehashi, J. Phys. Soc. Jpn. **50**, 1505 (1981); **50**, 3620 (1981).
[21]J. H. Samson, Phys. Rev. B **28**, 6387 (1983).
[22]Y. Kakehashi and P. Fulde, Phys. Rev. B **32**, 1595 (1985).
[23]T. Ogawa and K. Kanda, Z. Phys. B **30**, 355 (1978).
[24]A. M. Oleś, Phys. Rev. B **28**, 327 (1983).
[25]H. Takano and A. Okiji, J. Phys. Soc. Jpn. **50**, 2891 (1981).
[26]Y. Takahashi and K. Usami, J. Phys. Soc. Jpn. **51**, 2450 (1982).
[27]E.-N. Foo and H. Amar, Phys. Rev. Lett. **25**, 1748 (1970).
[28]M. Plischke and D. Mattis, Phys. Rev. B **7**, 2430 (1973).
[29]M. Sako and M. Shimizu, J. Phys. Soc. Jpn. **40**, 974 (1976).
[30]Y. Kakehashi, J. Phys. Soc. Jpn. **50**, 2251 (1981).
[31]L. N. Bulaevskii and D. I. Khomskii, Fiz. Tver. Tela (Leningrad), **14**, 3594 (1972) [Sov. Phys.—Solid State, **14**, 3015 (1973)]; Phys. Lett. **41A**, 257 (1972).
[32]S. A. Werner and A. Arrott, Phys. Rev. **155**, 528 (1967).
[33]Y. Kakehashi, J. Phys. Soc. Jpn. **50**, 1925 (1981).
[34]Y. Kakehashi, J. Phys. Soc. Jpn. **50**, 2236 (1981).
[35]D. G. Pettifor, J. Phys. F **8**, 219 (1978).
[36]U. K. Poulsen, J. Kollár, and O. K. Andersen, J. Phys. F **6**, L241 (1976).
[37]Y. Kakehashi, J. Phys. Soc. Jpn. **50**, 792 (1981), Table I.
[38]Y. Kakehashi and J. H. Samson (unpublished).